Validation of an Optical Microplate Label-Free Platform in the Screening of Chemical Libraries for Direct Binding to a Nuclear Receptor

Laura Vela,[1] Peter N. Lowe,[2] John Gerstenmaier,[3] Lance G. Laing,[3,] Julie B. Stimmel,[4] Lisa A. Orband-Miller,[4] and Julio J. Martin[1]*

[1]Screening and Compound Profiling, GlaxoSmithKline, Tres Cantos, Spain.
[2]Biomolecular Interactions Consultancy, Hertford, United Kingdom.
[3]SRU Biosystems, Inc., Woburn, Massachusetts.
[4]Screening and Compound Profiling, GlaxoSmithKline, Research Triangle Park, North Carolina.
**Present address: LGL Consulting, Belmont, Massachusetts.*

ABSTRACT

Optical microplate-based biosensors combine the advantages of label-free detection with industry-standard assay laboratory infrastructure and scalability. A plate-based label-free platform allows the same basic platform to be used to quantify molecular interactions of macromolecules and to screen and characterize drug-like small-molecule interactions. The ligand-binding domain of orphan estrogen-related nuclear receptor-γ (ERRγ) is utilized, as a model system of a challenging type of target, to illustrate the rapid development and utility of a range of biochemical assay formats on these biosensors. Formats in which either the domain, or a peptide derived from its cognate corepressor, RIP140, were immobilized were utilized. The direct binding of small drug molecules to the domain was characterized using immobilized domain. Subsequent addition of peptide distinguished whether compounds acted as either antagonists of peptide binding, or as agonists promoting a ternary complex. The format with peptide immobilized gave a more sensitive procedure for establishing the effect of compounds on the domain–peptide interaction. Using a direct-binding format, a diverse chemical library of 1,408 compounds in DMSO was screened for ability to bind to biosensors coated with ERRγ ligand-binding domain. Hits were then characterized using the other biosensor assay formats. The standard requirements for a full primary screening campaign were fulfilled by the acceptable hit-rate, quality-performance parameters, and throughput of the direct-binding assay format. Such a format allows direct screening of targets, such as orphan receptors, without the requirement for prior knowledge of a validated ligand.

INTRODUCTION

The universal principle of the action of drugs was enunciated in 1908 by Paul Ehrlich "*Corpora non agunt nisi fixate*" (a drug will not work unless it is bound). Most of today's primary screens pursue compounds that modulate the function of a target protein, and thereby provide indirect evidence of test compound binding. Direct binding as a primary screening procedure has hitherto been limited by access to suitable technologies.

The classical approach to drug discovery relies on the precise definition and formal validation of a few selected targets. In contrast, a chemical-genomics approach is based on genome-wide definition of many targets followed by compound screening and complete biological validation of a few targets using the identified tool compounds. However, 40% of human genes have no known ligand or defined molecular function.[1] The challenge to the expansion of therapeutic targets resides on the rapid definition of automated drug screening assays for large numbers of diverse classes of proteins. Screening methodologies looking directly at the binding of a compound to a given protein constitute a tractable solution to this end.

A wide variety of different direct binding label-free methodologies have been developed and adapted for use in research.[2–13] Current HTS technologies are almost all based on industry-standard microplates. Traditional label-free approaches such as ITC and surface plasmon resonance (SPR) do not comply with this architecture.[3,6–8] However, the recently commercialized photonic crystal-based biosensors are manufactured in standard microplate formats of 96, 384 and 1,536 wells.[9–13] These microplates can be read in easy-to-use benchtop plate readers, thereby forming a simple sensitive biosensor system, fully compatible with standard liquid and microplate handling automation. Biomass changes at the biosensor surface cause alterations in local refractive index (as with SPR), detected by precisely measurable shifts in the peak wavelength value (PWV) of sensor-specifically reflected light.

These plate-based biosensors potentially constitute a versatile platform for chemical compound screening in the pursuit of new therapies in both biochemical and cell-based applications. Such applications span from the screening of compound libraries to hit (in)validation, and mechanistic pharmacology of leads and from agonist trafficking to receptor panning.[4,9–13]

ABBREVIATIONS: b-RIP, biotinylated peptide derived from RIP140; CV, coefficient of variation; ERRγ, estrogen-related receptor gamma; LBD, ligand-binding domain; PWV, peak-wavelength value; SD, standard deviation; SPR, surface plasmon resonance; ΔPWV, the change in peak-wavelength value.

DOI: 10.1089/adt.2010.0345

Estrogen-related receptor gamma (ERRγ; NR3B3) is a member of the nuclear receptor superfamily. It is an orphan nuclear receptor that has no known natural ligand. Even with the similarities between ERRγ and the estrogen receptors to date, there is no detectable binding of estradiol or any other estrogen-like compounds. ERRγ tissue expression profiles and role in cardiac metabolism have been reported[14,15] as well as ERRγ interaction with coactivators and repressors such as the corepressor RIP140 (nuclear receptor-interacting protein 1) protein.

This article is intended as a demonstration of a strategy for prosecution of an orphan nuclear receptor, providing the basic biochemical tests of target activity using ERRγ on a photonic crystal biosensor platform. Direct-binding methods had not previously been pursued on ERRγ, though SPR studies on nuclear receptor ligand-binding domains have been reported.[16–18]

In the present article, we describe the validation of photonic crystal label-free methodology for biochemical applications using, as a model protein, the ligand-binding domain of ERRγ. This protein domain has no catalytic activity but retains the ability to bind RIP140, or a peptide derived from RIP140, as used in the studies here. Assay formats, in which either ERRγ ligand-binding domain (LBD) or RIP140 peptide has been immobilized on biosensors, were compared and used to characterize the activity of ERRγ LBD ligands, including known agonists and antagonists of RIP140 binding.

This work shows how plate-based biosensors can be readily utilized to set up a variety of assays either for primary identification of ligands or for their characterization. A key aim was to validate procedures that could be applied to targets that might be devoid of any defined ligand and, thus, demonstrate the potential of label-free to make such targets more accessible. An assay that measured direct label-free binding of small molecule compounds to the ERRγ LBD was used to demonstrate a range of biochemical characterizations. These included measurement of concentration dependency of binding, affinity, stoichiometry, kinetics, and specificity, all of which can be valuable for secondary screening and mechanistic analysis. This assay was then validated as a primary screening tool, through application to a subset of the full GSK screening library, consisting of 1,408 diverse small molecules in 384-well microplates. Additional assay formats are described that measure the interaction between the target receptor and its cofactor peptide. These would give mechanistic information on compounds active in a direct-binding screen, but would also be capable of directly screening for compounds with agonist or antagonist properties.

MATERIALS AND METHODS

Sensor Plates and Reader

GA-3 and SA1 BIND biosensor microplates (96- and 384-well) obtained from SRU Biosystems (Woburn, MA, USA) were read on a BIND Reader (SRU Biosystems). GA-3 sensor wells are coated with a high-density three-dimensional matrix with aldehyde functionalities. This allows direct coupling of proteins, via amino groups, for example, of lysine residues. SA1 wells have a lower density surface, prederivatized with streptavidin.

Proteins, Peptides, and Tool Compounds

Purified human ERRγ LBD (M_r 26400; 14.8 mg/mL in 25 mM Tris/HCl, pH8.0, 150 mM NaCl, 5 mM dithiothreitol, 2 mM EDTA, and 5% glycerol) nuclear receptor fragment was a kind gift from Tom Consler, GSK. This was obtained by expression in *E. coli* strain BL21(DE3) of a sequence encoding an amino-terminal modified polyhistidine tag fused in frame to a sequence encoding the ligand-binding domain (residues 229–458), subcloned into the pRSETa expression vector. Residues 372–392 of RIP140 peptide in native (RIP) and biotinylated (b-RIP) forms[19] were obtained from Synpep. 4-hydroxytamoxifen (M_r 388, clogP 5.69), an antagonist of ERR function[20] and of RIP peptide binding to ERRγ (henceforth called Antagonist), and GSK9089 (M_r 311, clogP 3.48), an agonist of RIP peptide binding to ERRγ[19] (henceforth called Agonist), were obtained from GSK.

Immobilization of ERRγ LBD and Peptide to Sensor Plates

After washing in 50 mM Hepes, pH 7, 50 mM KCl, 1 mM EDTA (Assay Buffer), GA3 biosensors were filled with ERRγ LBD (200 μg/mL, unless otherwise indicated) in Assay Buffer, for 96 wells, 50 μL; for 384 well 20 μL. After 1 or 18 h, the plates were washed with Assay Buffer, and the PWV read to monitor the amount of stably attached ERRγ LBD. The wells were emptied, and filled with 100 μL (96-well) or 50 μL (384-well) of 50 mg/mL SRU-G in Assay Buffer. SRU-G (from SRU Biosystems) is a proprietary small-molecule hydrophilic blocking reagent designed to inactivate remaining aldehyde groups. After 2 h, the wells were emptied and equilibrated with Assay Buffer. Biosensors were also prepared using exactly the same procedure, but omitting ERRγ LBD, to create a nontarget surface.

SA1 biosensors were treated similarly though filled with b-RIP (200 μg/mL, unless otherwise indicated) in Assay Buffer, using 50 μL for 96 wells and 20 μL for 384 wells. After 20 min, the plates were washed with Assay Buffer, and the PWV read to monitor the amount of biotinylated-RIP (b-RIP) bound. Control wells were also created in which the streptavidin surface had been preblocked with biotin, before adding b-RIP.

Both aldehyde-immobilized nuclear receptor and streptavidin immobilized b-RIP peptide formats proved to be stable on storage at 4°C, allowing batches of plates to be uniformly coated with target and stored for several days before use.

Ligand Interactions on Sensor

Small molecules and RIP peptide binding were used to test the activity of immobilized ERRγ LBD. ERRγ LBD was used to test the b-RIP surface. Typically, in the first step a baseline reading was recorded on a GA3 sensor coated with ERRγ LBD, prepared as described above, and equilibrated with 50 μL (96-well) or 25 μL (384-well) of Assay Buffer. In a second step, an equal volume of RIP peptide or small molecule each dissolved in Assay Buffer was then added, and the time-course of signal change was recorded until equilibrium was attained. In practice, various minor modifications were made to suit specific experiments. In particular, for samples containing DMSO in some experiments, wells were pre-equilibrated in Assay Buffer

containing DMSO, such that when the sample was added there was no change in the concentration of DMSO. In some experiments, Assay Buffer was supplemented with 2 mM CHAPS.

Binding Data Analysis

K_ds and responses at saturation were estimated from dose–response data by curve fitting of the equilibrium ΔPWV response at each ligand concentration to a 1:1 binding model that accounts for ligand depletion (Eq. 1). S is the measured ΔPWV, A_o is the total concentration of Ligand and B_o is the total apparent concentration of Target. S_{min} is the measured ΔPWV in the absence of Ligand, and S_{max} is the measured ΔPWV when all Target is complexed with Ligand, that is, at saturating A_o. This assumes that A gives no response itself, and gives no response other than through formation of AB complex, and that the concentration of the immobilized target can be taken to be that as if it were uniformally distributed within the assay volume. This simplification had previously been experimentally validated in similarly heterogeneous SPA Bead assays[21] and also with BIND assays using standard ligands and targets such as carbonic anhydrase[11,22]

$$S = S_{min} + (S_{max} - S_{min})([AB]/B_o), \quad (1)$$

where $[AB] = \dfrac{(K_d + A_0 + B_0) - \sqrt{(K_d + A_0 + B_0)^2 - 4 \times A_0 \times B_0}}{2}$.

Stoichiometries were calculated from the estimated responses at saturation based on the ratio of those to PWV response obtained by the immobilized target, with the assumption that the PWV response per unit mass of protein and bound ligand are identical.

In some experiments, nonspecific responses likely caused by combinations of bulk refractive index differences and of nonspecific binding were present. These could generally be modeled as a linear response with ligand concentration. So, the total BIND ΔPWV (S) is represented by:

$$S = S_{min} + (S_{max} - S_{min})([AB]/B_o) + A_o \times Slope, \quad (2)$$

where Slope is the gradient of the linear nonspecific response. Thus, a curve fit of the measured ΔPWV response at each ligand concentration to this model yields the additional parameter, Slope.

Screening of Chemical Library and Data Analysis

The screening of a small-molecule diversity compound set of 1,408 compounds was performed on 384-well GA3 biosensors (each in duplicate), either coated with ERRγ LBD or with a nontarget surface, prepared as described above (see Protocol in *Table 1*). Plate washing was performed with an automated plate-washer. Liquid additions were achieved using a 384-well head on a Biomek FX robot from Beckman Coulter. After each plate was washed and equilibrated in 22.5 μL (384-well) of assay buffer, a baseline reading was obtained. It was removed from the reader, and 2.5 μL of compound solution was added and mixed. The plate was read for 5 min to give a short time-course. Data were base lined to an average of two or more readings before compound addition.

Compound solutions (100 μM in 10% DMSO) were prepared in a 384-well stock-plate by a 1 in 10 dilution of a 1 mM stock in 100% DMSO into Assay Buffer. Column 6 was reserved as a low signal control in which compound was replaced with DMSO alone. Column 18 was reserved for high signal controls (100 μM in 10% DMSO): Rows 1–8 contained Antagonist and Rows 9–16 contained Agonist. Additionally, 16 randomly distributed wells on each well had test compounds omitted and replaced by spikes of Agonist and Antagonist giving final assay concentrations of either 1 or 10 μM, each in quadruplicate. Note that as the Assay Buffer did not contain DMSO, addition of compound caused a 1% DMSO mismatch and hence a baseline shift.

PWV shifts at equilibrium were recorded by EMS and processed with an Activity Base® (IDBS) template to normalize compound responses with respect to the two standard compounds used as reference, that is, Agonist and Antagonist. Both raw and normalized data

Table 1. Direct-Binding Assay Protocol Table for 384-Well GA3 Biosensor

Step	Parameter	Value	Description
A. Immobilization of ERR Target			
1	Equilibrate sensor	20 μL	Immobilization buffer
2	Baseline PWV reading		
3	Empty and replace with ERR	20 μL	200 μg/mL
4	Incubate	1 h	Ambient temperature
5	Empty, wash and replace with buffer	20 μL	
6	PWV reading	1 min	
7	Empty and replace with SRU-G	50 μL	50 mg/mL
8	Incubate	1 h	
9	Empty, wash and replace with buffer	22.5 μL	
10	PWV reading		
11	Seal plates and store for use		

Step Notes

1. Wash 3 times with 384-well plate washer.
2. As many time points as needed to reach a plateau (*i.e.*, %CV lower than 5).
3. Empty manually by inversion or by centrifugation of inverted sensor. Control wells without ERR can be included.
4. Time-course of changing PWV can be optionally followed.
5. Wash with 384-well plate washer.
6. Difference between PWV in Step 6 and Step 2 quantifies mass of ERR immobilized.
7. Dissolved in Assay Buffer.
9. Assay Buffer, containing DMSO at same concentration as samples to be tested.
10. Difference between PWV in Step 10 and Step 6 quantifies blocking efficiency.
11. Ambient for use within 4 h, otherwise 4°C.

Table 1. (Continued)

Step	Parameter	Value	Description
B. Binding Assay			
1	Equilibrate sensor on reader	10 min	Ambient temperature
2	Baseline PWV reading	1 min	Ambient temperature
3	Compound and control solutions (intermediate compound plates)	20 µL	In Assay Buffer
4	Add compounds and controls from compound plates to assay sensor plates	2.5 µL	Ambient temperature
5	PWV reading	10 min	Time-course

Step Notes

1. Remove seal 30 min before use. Time-course of PWV can be followed to confirm equilibration.
2. As many time points as needed to reach a plateau (*i.e.*, %CV lower than 5).
3. Prepare dilutions such that [DMSO] matches that in Assay Buffer. Good matching is critical.
4. Mix once. Time-course of changing PWV is followed from zero time. In this protocol the compound was diluted 1:10 into the assay. 1:1 dilution, for example, 25 µL compound to 25 µL buffer in the well, can be used.
5. Measure ΔPWV as difference between PWV in Step 5 and Step 2.

CV, coefficient of variation.

were posted to a database for subsequent retrieval and analysis. Activity thresholds for hit identification were set as three times the standard deviation of the sample population after outlier removal.

Dose–response curves (final concentration from 50 µM in doubling dilutions) for actives were performed on both ERRγ LBD and nontarget surfaces. The functional effect of actives on binding of ERRγ LBD to RIP peptides was monitored on b-RIP/streptavidin sensors with about 200 picometer (pm) of b-RIP bound. Controls were treated the same but with no b-RIP added. The 10 µM compound, 10 µM standard Agonist or Antagonist, or 0.1% DMSO were pre-incubated with 1.25 µM ERRγ LBD for 10 min before adding 50 µL of the mixtures to both b-RIP-coated and control wells.

RESULTS

Immobilization and Activity of ERRγ LBD

The first step is the immobilization of one binding component onto the biosensor, which can be achieved using a variety of chemistries. Immobilization was achieved here via covalent linkage of amines (lysine residues) to a high-density aldehyde-derivatized surface through a one-step procedure whose effectiveness was monitored in real-time. The standard microplate format allows many conditions to be tested in parallel for economic optimization. In this example, time and concentration of target were the main variables that were altered, as the majority of immobilization occurred at <1 hr in a standard buffer at neutral pH (*Fig. 1*). The same maximum coating density of ERRγ LBD (ΔPWV of 9,000 pm) was achieved in both 96-well (*Fig. 1A*) and 384-well (*Fig. 1B*) plates. Simultaneous addition to all wells and immobilization to saturation minimized well-to-well variability, giving coefficient of variations of about 2%.

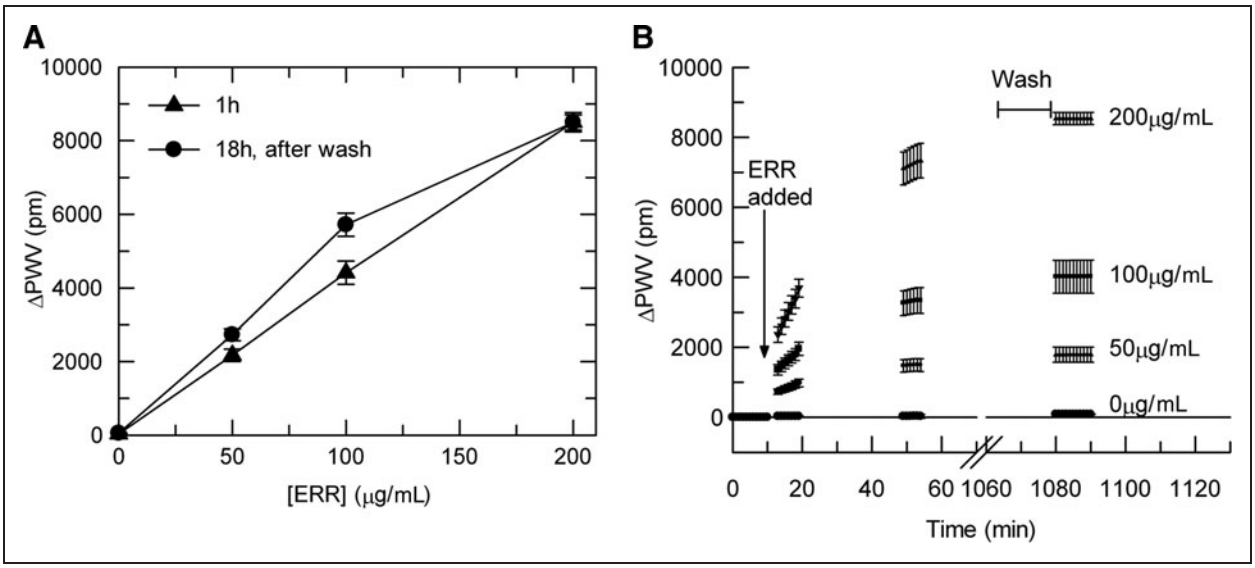

Fig. 1. Immobilization of ERRγ ligand-binding domain (LBD) on GA3 sensors. The 96-well and 384-well GA3 sensors were equilibrated in Assay Buffer and a baseline BIND response measured. The well contents were replaced with 0, 50, 100, or 200 µg/mL ERRγ LBD in Assay Buffer, and the time-course of BIND response measured over a period of 18 h. The plate was then washed in Assay Buffer and the BIND response recorded. **(A)** ΔPWV ± standard deviation (SD) ($n = 24$) at 1 h and after final wash on a 96-well sensor at each concentration of ERRγ LBD. **(B)** The time-course of ΔPWV ± SD ($n = 24$) at each concentration of ERRγ LBD on a 384-well sensor.

To determine the functional activity of the immobilized nuclear receptor, it was probed with low-molecular-weight tool compounds, Agonist (GSK9089) and Antagonist (4-hydroxytamoxifen). Compound binding was found to be broadly proportional to the level of target immobilized on both 384-well (data not shown) and 96-well (*Fig. 2A*) plates. The stoichiometry of Agonist binding was close to 1 mol/mol of immobilized target (*Fig. 2B*), suggesting that the nuclear receptor is fully functional. The Antagonist bound with a stoichiometry that appeared to be >1:1 and which declined at higher target density (*Fig. 2B*); the latter effect likely due to higher density of immobilized ERRγ LBD reducing nonspecific binding.

Direct Binding Affinity Measurement of Small Molecules to Immobilized ERRγ LBD

Direct binding of Agonist and Antagonist to the target ERRγ LBD surface (*Fig. 3*) gave biphasic dose–response curves, interpreted as being a combination of 1:1 saturable binding and a linear nonspecific response. Curve fitting quantified the functional concentration of target in the well. The data from Agonist and Antagonist curves binding to ERRγ LBD surface were self-consistent, giving an ERRγ LBD target concentration of 6 μM. K_d values could not be determined as the experiments were at the tight-binding limit. However, by comparing experimental data with simulated curves with the ERRγ LBD concentration set at 6 μM, the K_d was assessed to be <100 nM for both Agonist and Antagonist interactions. The reported K_d for Antagonist obtained using a scintillation proximity assay was 35 nM,[19] consistent with our data. For Agonist, others reported the EC_{50} as 2,000 nM.[19] This apparent weaker binding than we observed is likely to be due to the use of competition assays,[19] rather than direct binding employed here.

At concentrations above 2 μM, both Agonist and Antagonist showed a weak, nonspecific, nonsaturable response on a nontarget surface of 8 pm/μM that was much greater than that seen on the ERRγ LBD surface of 2–3 pm/μM (*Fig. 3*). Thus, the nontarget surface proved to be a poor reference surface, a situation quite frequently seen with immobilized targets.

Agonism and Antagonism of Binding of RIP to Immobilized ERRγ LBD

Sufficient amounts of ERRγ LBD could be immobilized on the sensor to permit direct-binding measurements of small molecules or of RIP peptide or of ternary complex formation. The time-courses of binding and the equilibrium binding levels could be monitored for each species. Such experiments were performed either by adding RIP then compound or vice versa.

Figure 4A shows a time-course in which binding of either Agonist or Antagonist, or a control without compound, was followed by addition of cofactor peptide. Whereas the binding of small molecules to most simple targets is usually sufficiently fast that the full response is seen within the mixing time, the kinetics of binding to ERRγ LBD were slow and the time-course was clearly visible (*Fig. 4A*). This might be related to slow conformational changes often associated with binding to nuclear receptor ligand-binding domains.[16,23] In the control, RIP peptide binding is seen as a time-dependent increase in signal. Prebinding of Agonist resulted in a doubling of the response to RIP addition, whereas prebinding of Antagonist abrogated binding of RIP.

Figure 4B shows a time-course in which binding of the cofactor peptide was seen as a slow increase in PWV signal, reaching an equilibrium level after about 20 min. Subsequent addition of Agonist caused a very substantial increase in signal, making this format very sensitive to agonists. The PWV shift was due to the combination of the signal from the Agonist binding, and RIP binding. Addition of an Antagonist to the receptor–peptide complex resulted in a decrease in signal to a level compatible with the signal due to the ERRγ LBD:Antagonist complex in the absence of any RIP at all.

The impact of Agonist and Antagonist on RIP binding to immobilized ERRγ LBD were then examined in more detail. *Figures 4C* and *D* show the amount of Antagonist (*Fig. 4C*) or Agonist (*Fig. 4D*) bound at varying concentrations of each compound in the absence of RIP and the further response when RIP was subsequently added. The response to RIP correlated with the amount of compound already bound in the expected manner for Antagonist and Agonist, respectively.

The kinetics of RIP binding were dependent upon the level of immobilized ERRγ LBD (data not shown). At low levels of ERRγ LBD, binding of 5–10 μM RIP occurred very quickly (k_{obs} ca 1 min^{-1}), but at saturating levels of ERRγ LBD, slower kinetics were seen (k_{obs} ca 0.17 min^{-1}). As exemplified in *Figure 4E*, using either 96- or 384-well plates, it was possible to obtain large numbers of highly reproducible kinetic time-courses in parallel and to obtain curve fits to yield rate constants. The fits shown in *Figure 4E* were obtained with a single exponential; slightly better fits were obtained to a double exponential (data not shown), with an initial fast rate (k_{obs} = 1.4 min^{-1}, amplitude of ~30% of total), followed by a slower phase (k_{obs} = 0.19 min^{-1}, amplitude ~70% of total). This is consistent with the second slower phase being due to mass transfer limitation at high ERRγ LBD. Agonist predominantly increased the amplitude, rather than the rate of association (data not shown). Antagonist-induced dissociation could be fit to a single exponential decay with a dissociation rate constant of 0.63 min^{-1} (*Fig. 4E*, inset)

Titrations with RIP gave dose–response curves that could be fitted to 1:1 binding isotherms, without a requirement for any nonspecific binding component (*Fig. 4F*). The K_d for RIP binding to immobilized ERRγ LBD was about 13 μM, with a predicted maximum stoichiometry of 0.82 mol of RIP/mol of ERR. In the presence of Agonist, the K_d was lowered to about 6 μM, with a stoichiometry of 0.73 mol of RIP/mol of ERRγ LBD. In the presence of Antagonist, the K_d was >100 μM and RIP binding was largely blocked confirming the low level of nonspecific binding in this format.

Immobilization of b-RIP, and ERRγ LBD Binding to the Surface

In an inverted format, capture of ERRγ LBD onto b-RIP peptide immobilized on a streptavidin sensor demonstrated another method of studying the pharmacology and mechanisms of action of compounds. This format has the advantage of giving a very large increase

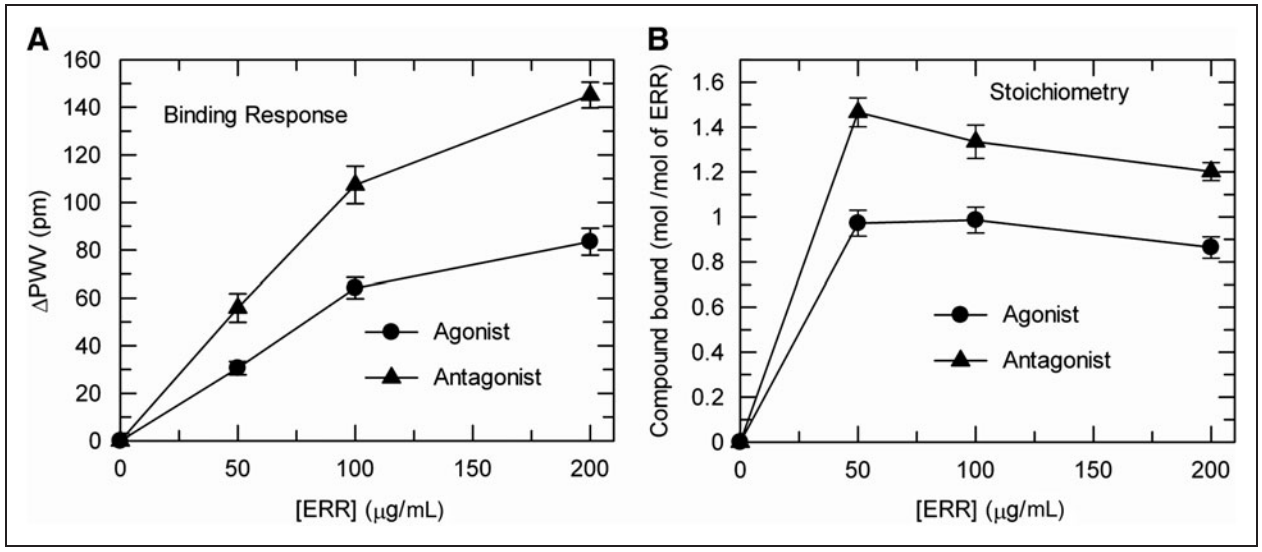

Fig. 2. Probe of functional activity of immobilized ERRγ LBD. ERRγ LBD, at 0, 50, 100, or 200 μg/mL, was immobilized on a 96-well GA3 sensor for 1 h, blocked with SRU-G, and equilibrated in Assay Buffer, and a baseline BIND response was measured. Either Antagonist or Agonist was then added to each well to give a final concentration of 10 μM, and the time-course of BIND response recorded. Specific binding response reached equilibrium within 4 min after addition. **(A)** shows these as ΔPWV ± SD (n = 8). The readings were referenced to blank wells, which had no target receptor immobilized. **(B)** The measured stoichiometries calculated from the BIND responses from the immobilized ERRγ LBD and from compound binding, and the relative M_r of each compound and of ERRγ LBD.

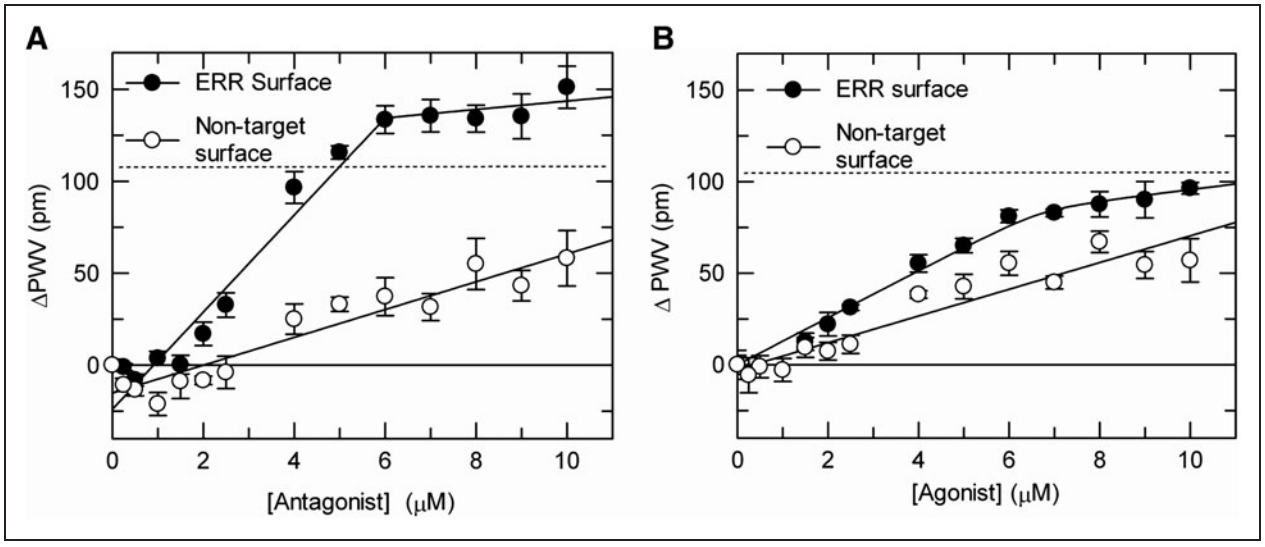

Fig. 3. Direct binding of small molecule ligands to immobilized ERRγ LBD. Wells of a GA3 sensor were either uncoated (nontarget surface) or coated with ERRγ LBD (final level after wash 9,300 pm) (ERRγ LBD surface) and blocked with SRU-G. After equilibration in Assay Buffer, dilution series of either Antagonist **(A)** or Agonist **(B)** were added to the indicated final concentrations to both ERRγ LBD and nontarget surfaces and the consequent ΔPWV recorded. The graphs show the curve fits for the ERRγ LBD surface data to Equation 2 with a total target concentration of 6 μM, and for the nontarget surface to just a linear nonspecific response. The fitting parameters (±standard error) on the ERRγ LBD surface for the Antagonist were a slope of the nonspecific response of 2 ± 3 pm/μM of compound, and a max response corresponding to measured stoichiometries of 1.1 ± 0.2 mol/mol. For the agonist they were 3 ± 1 pm/μM and 0.6 ± 0.1 mol/mol, respectively. The K_d values were <100 nM, but poorly defined. For both compounds, the slopes of the nonspecific response on the nontarget surfaces were 8 ± 1 pm/μM. The dotted line represents calculated response for a stoichiometry of 1.0.

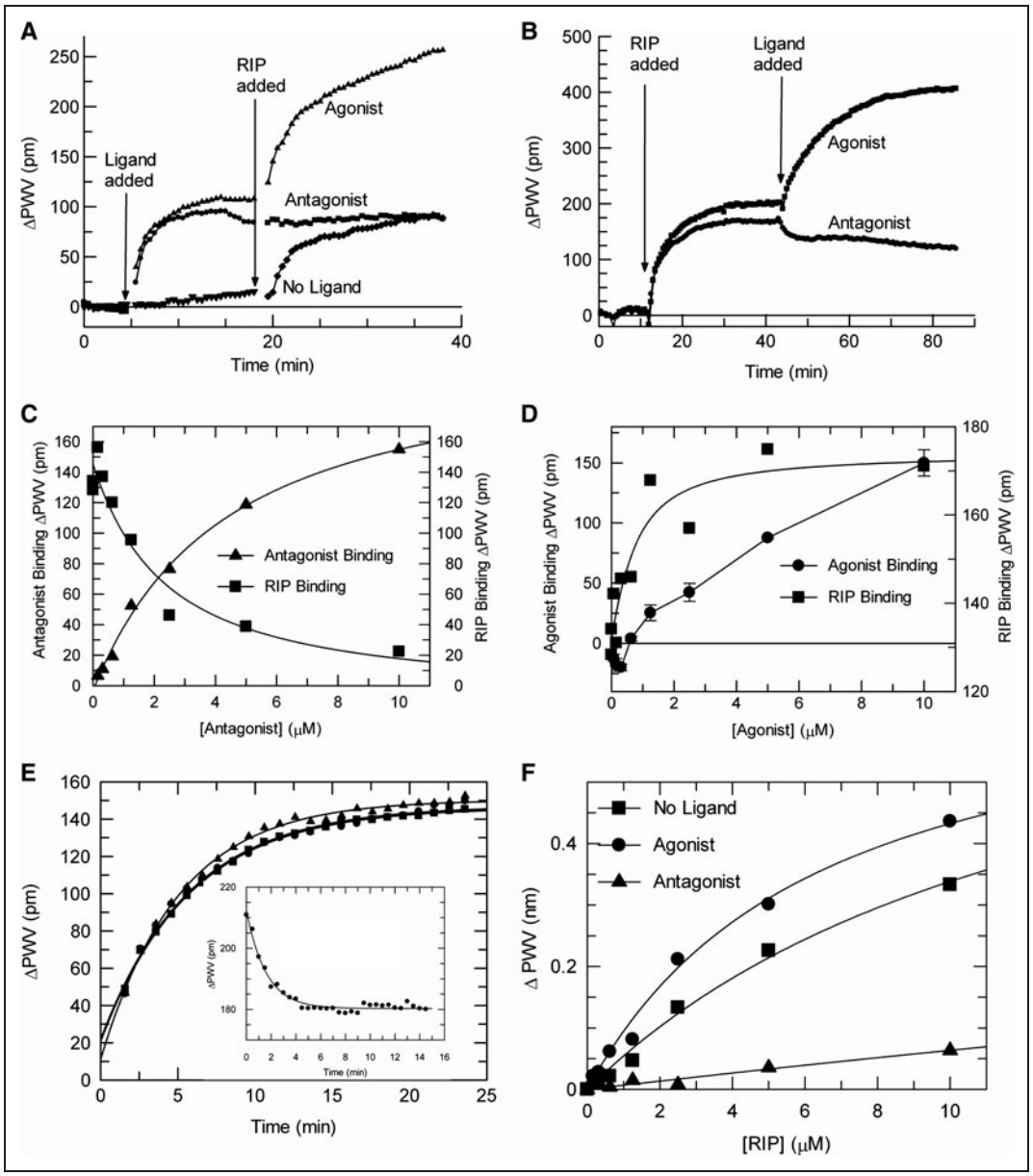

Fig. 4. RIP- and compound-binding to immobilized ERRγ LBD. **(A, B)** Wells of a GA3 sensor were coated with ERRγ LBD (final level after wash 6,500 pm), blocked with SRU-G, and equilibrated in Assay Buffer, and a baseline was taken. Then, the time-courses of BIND responses were recorded when Agonist or Antagonist (final concentration 10 μM) and RIP (final concentration 2 μM) were added in two different orders. In **(A)**, Agonist, Antagonist, or DMSO (no ligand) was added, followed by RIP to all wells. In **(B)**, the order was reversed and RIP was added to all wells, followed by Agonist, Antagonist, or DMSO (no ligand). **(C, D)** Effect of compound concentration on its binding and subsequent RIP binding. Wells of a 384-well GA3 sensor were coated with ERRγ LBD (final level after wash 8,900 pm), blocked with SRU-G, and equilibrated in Assay Buffer, and a baseline was taken. Then, a dilution series of either Antagonist **(C, ▲)** or Agonist **(D, ●)** were added and the equilibrium BIND response measured. Subsequently, RIP was added to a final concentration of 2 μM and, at equilibrium, the change in BIND response measured (■). **(E)** Kinetics of RIP on immobilized ERRγ LBD. A 384-well GA3 sensor was coated with ERRγ LBD, blocked with SRU-G, and equilibrated in Assay Buffer, and a baseline was taken. RIP was added to nine wells to a final concentration of 5 μM and the time-course of binding fitted to a single exponential, with rate constants of 0.17 ± 0.02 min^{-1} ($n = 9$) For clarity, data from just three wells are shown in **(E)**. Double-exponential fits (not shown) accounted better for the higher rates in the first minutes. In a separate experiment, the time-courses of dissociation of RIP, induced by addition of Antagonist, was fitted to a single exponential of rate constant 0.63 min^{-1} (inset). **(F)** Equilibrium BIND responses for a dilution series of RIP in the presence of DMSO alone (No Ligand), Agonist, or Antagonist on immobilized ERRγ LBD were measured and fitted to a 1:1 binding model yielding K_d ± standard error of 13 ± 4, 6 ± 2 and >100 μM, respectively. The measured stoichiometries at saturating RIP were 0.8 ± 0.2 mol/mol with no ligand and 0.7 ± 0.1 mol/mol with Agonist.

in PWV due to the receptor's relatively high molecular weight. The model can also be used in situations where the target protein is not sufficiently active when directly immobilized.

Addition of a saturating concentration of b-RIP (5 μM) to a streptavidin sensor gave a robust signal of 360 pm shift in <10 min. Only specific capture of biotinylated peptide was seen, as judged by complete reduction of all binding by prior treatment with biotin. Addition of ERRγ LBD to this b-RIP biosensor surface gave a very robust response. However, this level of b-RIP capture was not optimal in terms of its interactions with ERRγ LBD. This was investigated in detail by first utilizing concentrations of b-RIP between 0.1 and 2 μM to create sensor surfaces with varying levels of b-RIP immobilization (15–160 pm PWV shift), and then characterizing the functional activity of each loading of b-RIP with a titration with ERRγ LBD. In each case, the time-courses of ERRγ LBD binding were recorded up to equilibrium and key data are shown in *Figure 5*. Multiphasic time-courses of ERRγ LBD binding were seen at higher levels of b-RIP immobilization, particularly with lower concentrations of ERRγ LBD, but were much less pronounced with subsaturated coatings of b-RIP and with higher concentrations of ERRγ LBD (*Fig. 5A*, and data not shown). The dose–response curve for equilibrium binding of ERRγ LBD onto this surface was biphasic. It was interpreted as being the combination of single-site saturable binding, together with a smaller, linear, increase, most evident at >2 μM-ERRγ LBD, due to nonspecific binding to the b-RIP surface (*Fig. 5B*). Curve fitting, based on this model, provided a K_d value of ~0.4 μM, which was independent of the density of immobilized b-RIP. A higher stoichiometry of binding, ~1.1 mol/mol, was achieved with a subsaturating level of b-RIP coating (38 pm) shift, as compared to 0.5–0.7 mol/mol on saturated b-RIP surfaces (legend to *Fig. 5B*). The lower stoichiometries observed when higher levels of RIP were used are likely due to steric constraints due to too dense packing. This result directed assay development toward reduced b-RIP loading conditions where sensitivity and ERRγ LBD activity was maximized.

As CHAPS had typically been incorporated into prior biochemical assays using ERRγ LBD, the effect of 2 mM CHAPS was examined on the time-courses and affinity. CHAPS caused an increase in rate of binding, but made the biphasic nature more pronounced (*Fig. 5A*). The final level of binding was almost unaffected. CHAPS showed a negligible effect on the K_d for ERRγ LBD binding to b-RIP regardless of the density of immobilized b-RIP (*Fig. 5B*). Subsequent experiments were all performed in the presence of 2 mM CHAPS.

This assay format was then validated by looking at the effect of adding 25 μM Agonist or Antagonist to wells from the previous experiment after equilibrium binding of ERRγ LBD had been achieved (*Fig. 5C*). Addition of Antagonist gave an 80% reduction in the ERRγ LBD signal when 1 μM ERRγ LBD was used. As ERRγ LBD concentration was increased, the reaction became less inhibited, consistent with their mutually exclusive binding. This was not affected by the level of b-RIP coating (*Fig. 5C*). In contrast, addition of 25 μM Agonist resulted in 20% and 15% increases in the ERRγ LBD signal on low and high levels of b-RIP coating, respectively. This was largely independent upon varying ERRγ LBD between 0.19 and 12 μM (*Fig. 5C*).

Agonism and Antagonism of the Binding of ERRγ LBD to Immobilized b-RIP

Utilizing this b-RIP-coated sensor format, the effects of low-molecular-weight compounds on the nuclear receptor's ability to interact with its effector peptide were examined in more detail (*Fig. 6*). The BIND technology allowed monitoring of the time to reach equilibrium as well as equilibrium binding. Several differences in surface density, timing, order of addition, and concentrations were tried (*Fig. 6*, and data not shown). The results demonstrate the simplicity of assay development with this technology, enabling the optimal dynamic range and equilibrium conditions to be obtained. For example, a comparison of *Figures 6A and B* exemplifies how sensitivity to Agonist can be altered by order of addition and timing. Procedures could also be optimized either to determine equilibrium binding and K_d (*Fig. 6C*) or to allow sensitive determination of EC_{50}s of both Agonist and Antagonist in a single procedure (*Fig. 6D*).

A dilution series of ERRγ LBD (between 0 and 12 μM) was preincubated alone, with 25 μM Agonist, or with 25 μM Antagonist, and then added to a b-RIP-coated sensor (*Fig. 6C*). The high compound concentrations ensured complete saturation of ERRγ LBD at all concentrations of ERRγ LBD used to generate the ERRγ LBD:bRIP titration curves. There was about a 35% increase in signal in the presence of agonist, suggestive of simultaneous binding of this agonist and RIP by ERRγ LBD. K_d for ERRγ LBD binding to b-RIP in the absence and presence of Agonist were measured at 0.26 ± 0.09 μM and 0.31 ± 0.12 μM, respectively (*Fig. 6C*).

A dilution series of Agonist or Antagonist (between 0 and 20 μM) was preincubated with 2.5 μM-ERRγ LBD and then added to a b-RIP-coated sensor (*Fig. 6D*). With Agonist, a maximal 59% increase in response was seen yielding an EC_{50} of 0.34 μM. With Antagonist, the signal was reduced with an EC_{50} of 0.48 μM. The total signal was maximally decreased by 80%, but the RIP-dependent component was 100% abolished, confirming that simultaneous Antagonist and RIP binding by ERRγ LBD was not possible. Additionally, the Antagonist does not appear to remove RIP-independent ERRγ LBD binding, consistent with that response being nonspecific.

Screening of 1,408 Compound Validation Set for Direct-Binding to Immobilized ERRγ LBD

Validation of the assay configuration for the discovery of low-molecular-weight compounds able to bind to the nuclear receptor was carried out by screening of a small chemical library of 1,408 compounds of random diversity (Protocol in *Table 1*). Physicochemical features (*e.g.*, molecular weight, cLogP, CMR, number of aromatic rings, number of heavy atoms, and Andrew's binding energy) of this compound set do not significantly differ from compounds within WDI and Sneader Drugs and Leads collections.[24] Thus, despite its small size, we expect that results and conclusions inferred from the behavior of this pilot compound set are not biased and can be extrapolated to larger random collections.

The assay validation compound set comprised four different 384-well plates, laid out such as to include space for appropriate

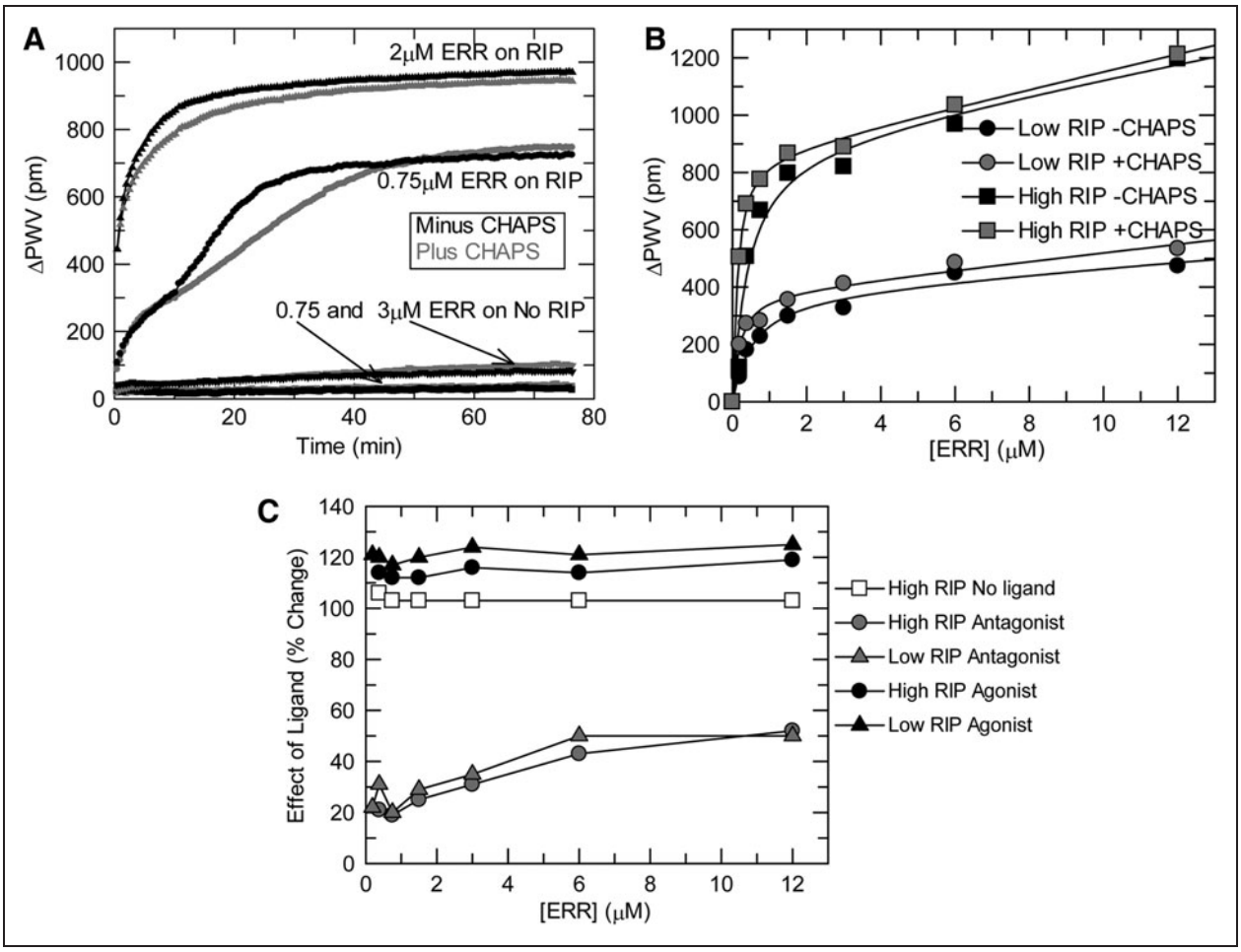

Fig. 5. ERRγ LBD binding to b-RIP immobilized on an SA1 biosensor. b-RIP (0.5 or 2 μM) was immobilized on SA1 plates to give low-density (ΔPWV of 38 pm) and high-density (ΔPWV of 163 pm) RIP surfaces. Replicate wells were equilibrated in the absence or presence of 2 mM CHAPS. Dilution series of ERRγ LBD in the respective buffer were added and the time-courses and equilibrium binding responses recorded. Immediately afterward, without washing, Agonist or Antagonist (final concentrations 25 μM) or DMSO as a no-ligand control were added to replicate wells and the time-courses were followed until a new equilibrium response was obtained. **(A)** The time-courses of binding of 0.75 or 3 μM ERRγ LBD on wells coated with 2 μM b-RIP or no b-RIP, in the absence and presence of CHAPS. **(B)** The equilibrium BIND responses at the indicated final concentrations of ERRγ LBD on low- and high-density RIP surfaces, in the absence and presence of CHAPS. The lines are curve fits to a model for single site binding with a linear nonspecific response. The K_d values obtained in the absence of CHAPS were 0.5 ± 0.2 μM (low RIP) and 0.4 ± 0.2 μM (high RIP). The K_d values obtained in the presence of CHAPS were 0.15 ± 0.05 μM (low RIP) and 0.09 ± 0.01 μM (high RIP). The BIND responses at saturating ERRγ LBD in the absence of CHAPS were 380 pm (low RIP) and 900 pm (high RIP) and in its presence were 380 pm (low RIP) and 850 pm (high RIP). These corresponded to measured stoichiometries of about 1:1 and 0.5:1 on low and high RIP surfaces, respectively. Slopes of nonspecific response function were 10–15 pm/μM with low RIP and 25–30 pm/μM at high RIP. **(C)** shows the effect of Agonist or Antagonist on the level of ERRγ LBD binding to RIP, in the presence of varying concentrations of ERRγ LBD. At each concentration of ERRγ LBD, the equilibrium responses obtained after addition of Agonist or Antagonist was used to calculate the percentage change caused by each ligand, relative to that of the DMSO control. The values obtained in the presence of CHAPS are plotted against each concentration of ERRγ LBD.

controls, and was screened in duplicate. As controls, wells with 1% DMSO alone (for compounds with 0% response) and 1% DMSO with Antagonist (for compounds with 100% response) were included. Additionally, as this was a validation procedure, some compound wells were spiked with Agonist or Antagonist. Each ERRγ LBD-coated sensor plate was quality controlled for nuclear receptor immobilization before compound addition (*Table 2*). The high uniformity was demonstrated by coefficient of variations of 2.3%–3.0% within, and of 0.7% between the 8 plates (*Table 2*). As key quality indicators of the screening process, we followed evolution of mean ΔPVWs and standard deviations of samples and controls (*Table 2* and *Fig. 7*). Z-prime robustness screen statistic was calculated from these two control types. All wells with spiked standard compounds were correctly identified. Correlation between duplicates was excellent with R-square correlation factors higher than 0.8 (*Fig. 7A*). Despite the small PWV changes associated with

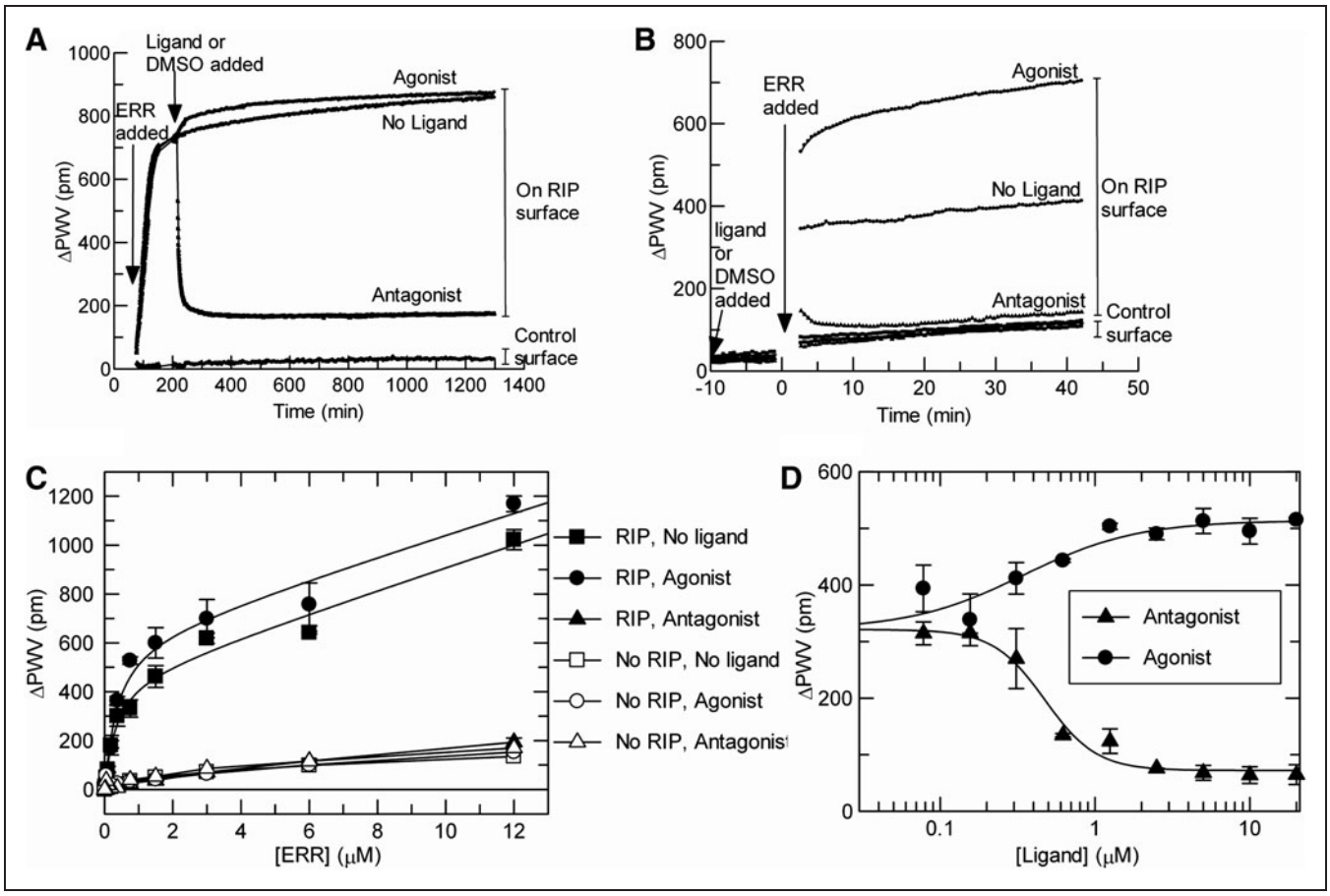

Fig. 6. Effect of Agonist and Antagonist on ERRγ LBD binding to b-RIP-coated sensors. **(A, B)** These show the effect of Agonist and Antagonist on the time-courses of ERRγ LBD binding to SA1 sensors coated with b-RIP (RIP) or uncoated (control), in the presence of 2 mM CHAPS. Two procedures were used. In **(A)**, the sensor was coated with 163 pm of b-RIP. 0.38 μM ERRγ LBD was added first and incubated long enough to reach near equilibrium binding before either 25 μM Agonist, or Antagonist or DMSO (no ligand control) were added. In **(B)**, the sensor was coated with 79 pm of b-RIP. 10 μM Agonist, Antagonist, or DMSO (no ligand control) were added, followed by addition of 2.5 μM ERRγ LBD. **(C)** SA1 sensor wells were untreated (control surface) or coated with 2 μM b-RIP (RIP surface), washed, and emptied. A dilution series of ERRγ LBD was made in the presence of a constant concentration of 25 μM Agonist or 25 μM Antagonist or DMSO (no ligand control), allowed time to bind and added to the empty wells. The time-courses of binding were followed. The graph shows the ΔPWV ± SD (n = 2) after 50 min at each [ERRγ LBD], and the fits to Equation 2, with the following parameters: K_d in the absence and presence of Agonist were 0.26 ± 0.09 μM and 0.31 ± 0.12 μM, respectively. Responses at saturation were 460 pm and 620 pm, respectively, and the slopes of nonspecific response function were 45 pm/μM for both. **(D)** Agonist and Antagonist titrations in presence of 2.5 μM ERRγ LBD. SA1 sensors were coated with 2 μM b-RIP, washed, and emptied. Dilution series of Antagonist or Agonist were each made in the presence of a constant concentration of 2.5 μM ERRγ LBD, allowed time to bind and added to the empty wells. The time-courses of binding were followed. The graph shows the ΔPWV ± SD (n = 2) after 40 min at each concentration of Ligand, and the fits to an EC_{50} logistic.

specific binding (~140 pm), standard deviations were kept very tight and Z-prime was maintained above 0.5 for all plates (*Table 2*). Moreover, the standard deviation among compound samples was not much greater than for controls (*Table 2*). Hence, the experimental procedure is suitable to cope with the variability due to possible mismatches in the concentration of DMSO across compound samples.

The time to reach equilibration for the standards was <5 min (*Fig. 4A*). To ascertain the stability of the plate and the signal with the compound set, one assay plate (353 compounds) was read after 15 min and again after 24 h. The responses (ΔPWV ± standard deviation [SD], $n = 8$) to the addition of No Ligand (low control), Antagonist or Agonist (high controls) were initially 134 ± 9 pm, 289 ± 13 pm, and 241 ± 19 pm, respectively. After 24 h, they were 140 ± 11 pm, 242 ± 16 pm, and 230 ± 37 pm, respectively. Thus, the low and high controls were quite stable for 24 h. The responses of the test compounds were also generally stable, with a correlation coefficient of 0.87 between the initial and 24 h readings. However, some compounds, particularly those with responses initially similar to that of the high controls, showed increased responses, and in some cases to a superstoichiometric level. This is consistent with time-dependent nonspecific binding (see Discussion). The assay time for

Table 2. Screen Parameters

Parameter	Plate Number							
	1	2	3	4	5	6	7	8
Immobilization ΔPWV ± SD (pm)	9,100 ± 290	9,090 ± 250	9,360 ± 210	9,090 ± 260	9,070 ± 250	9,030 ± 220	9,380 ± 280	9,230 ± 280
Immobilization CV (%)	3.2%	2.7%	2.3%	2.9%	2.8%	2.4%	3.0%	3.0%
Low control ΔPWV ± SD (pm)	120 ± 10	160 ± 10	130 ± 10	140 ± 10	130 ± 10	140 ± 10	130 ± 10	130 ± 10
Low Control CV (%)	6.5	5.4	7.5	5.3	5.2	6.4	6.5	7.8
High control ΔPWV ± SD (pm)	280 ± 10	330 ± 10	290 ± 10	340 ± 10	310 ± 10	360 ± 20	300 ± 10	320 ± 20
High Control CV (%)	2.4	4.4	4.5	4.1	4.2	5.8	4.6	4.8
Z′	0.72	0.60	0.55	0.67	0.67	0.59	0.62	0.62
Compounds ΔPWV ± SD (pm)	130 ± 20	170 ± 10	140 ± 20	160 ± 20	140 ± 10	150 ± 20	140 ± 20	140 ± 20

The uniformity of immobilization of ERRγ ligand-binding domain within each plate is shown as ΔPWV ± SD (n = 384) and as %CV. The uniformity between plates is 9,140 ± 70 pm (n = 8), with CV = 0.7%. Values are derived for standard calculations of Z′ using high (Antagonist with 1% DMSO) and low (1% DMSO) controls (n = 16 wells/plate). Data have been baselined to a time-point before addition of samples.

SD, standard deviation.

the rest of the compound set was fixed at 15 min after addition of compounds.

Screening Data Analysis

Primary screening results were analyzed by several criteria to determine a refined list of primary hits. At the first level, hits are identified as those compounds exhibiting a ΔPWV on the ERRγ LBD surface that is statistically different from the population of inactive compounds, that is, three times the standard deviation of samples in the absence of outliers. According to this initially applied criterion, a list of 140 compounds, representing 7% of the compounds on the four plates tested, was selected. Subsequent selection criteria were then employed to select for specific rather than nonspecific binding responses.

In general, nonspecific (false-positive) responses can come from bulk refractive effects such as solvent mismatches and from compounds with avidity to the sensor surface other than at a specific site on the target, such as many promiscuous or aggregating compounds. Potential nonspecific binding was indicated by four warning signals: (a) time-courses of binding that were much slower than the tight-binding standard Agonist and Antagonist, (b) measured binding stoichiometries on the ERRγ LBD surface that were significantly higher than those of the standard Agonist and Antagonist, (c) high signal with a nontarget surface as compared to that on a target surface, and (d) dose–response curves that do not fit a 1:1 binding isotherm. In this study, we eliminated a small number of compounds on the basis of super-stoichiometric binding, but the main selection criterion chosen was for those compounds that had a relatively higher signal on the target surface versus a control surface. Many compounds gave a PWV shift even in the absence of any target on the sensor surface, which were a combination of small DMSO mismatches and nonspecific binding. It was found that for almost all compounds there was a clear linear correlation between the responses on the ERRγ LBD surface and on the nontarget surface (*Fig. 7B*). Specific hits were therefore defined as those compounds that lie away from that linear correlation. To use a quantifiable estimator for hit cut-off, we calculated the selectivity ratio as the response in the Nuclear Receptor plate divided by the response in the Reference Plate (*Fig. 7C*). The selectivity ratio for samples is 0.7 ± 0.06 (mean ± SD), which was similar to that for DMSO alone. Hits falling above the 3 × SD threshold, within the corridor defined by inactive samples and Agonist and Antagonist controls, were picked up as putative specific hits. In summary, using the 3-level determination described above, 9 out of the 1,408 compounds screened were selected as initial hits, corresponding to a hit rate of 0.6% (*Fig. 7C*). These 9 compounds had the following physicochemical properties, quoted as mean ± SD (range): M_r, 372 ± 72 (243–483); clogP, 4.5 ± 1.3 (2.1–5.7); number of heavy atoms, 26 ± 7 (13–34); total polar surface area, 71 ± 31Å^2 (18–110 Å^2); number of aromatic rings, 3.0 ± 1.4 (1–5); calculated molar refractivity (cmr), 10 ± 3 (5.6–13.6)

Hit Follow-up by Direct Binding to Immobilized ERRγ LBD and Effect on Binding of ERRγ LBD to Immobilized b-RIP

Sample data for three compounds that typified the dose–responses seen for direct-binding to immobilized ERRγ LBD are shown in *Figure 8A*. Some did not show any response; some showed nonsaturable responses often with very high apparent stoichiometries and with larger responses on the nontarget surface. No compounds had the expected characteristics of a 1:1 binder to ERRγ LBD (*i.e.*, saturable binding with a signal of ~120 pm for a 350Mr ligand). When solid

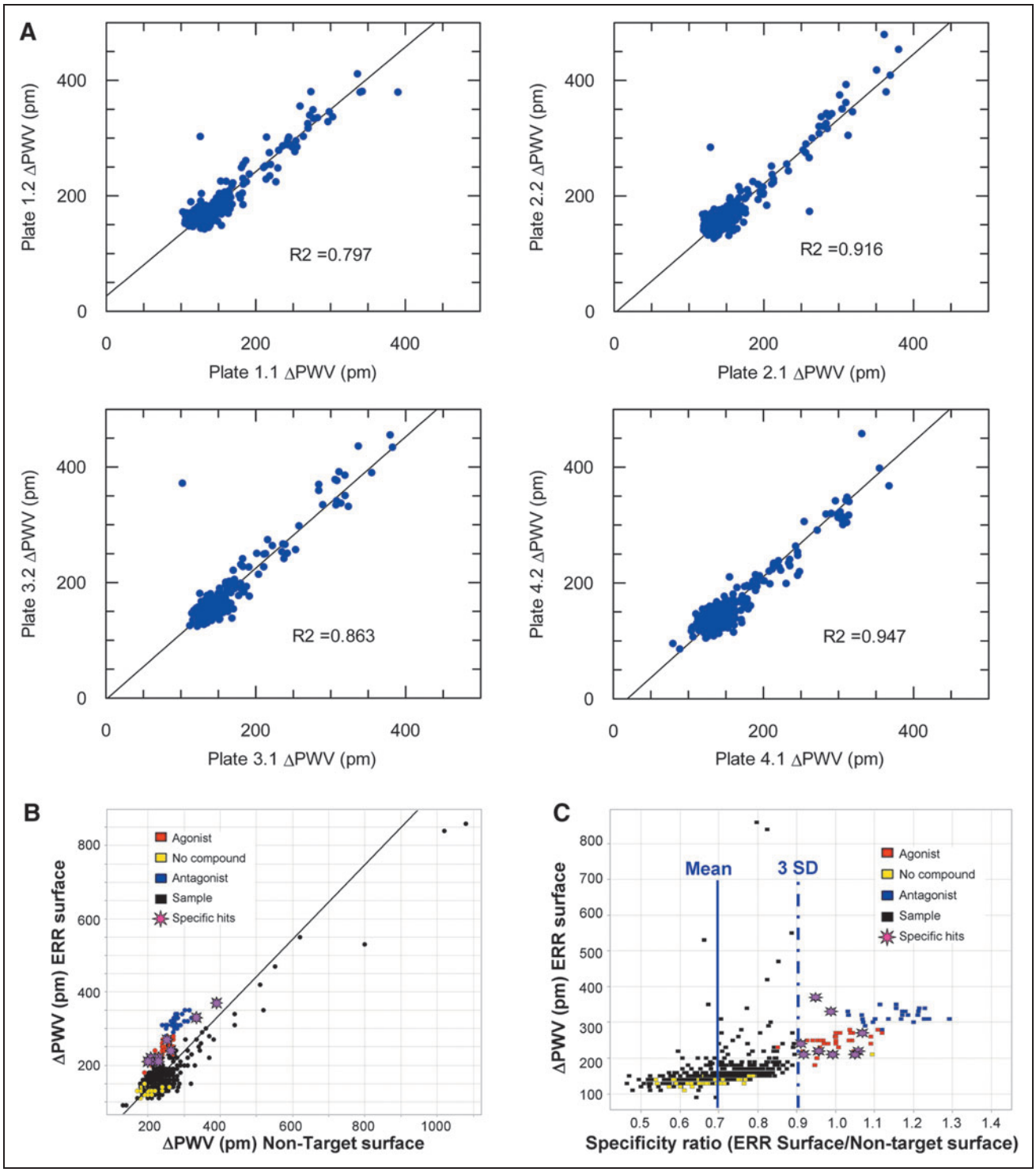

Fig. 7. Key quality and performance indicators and hit identification. **(A)** The correlations between four replicate sensors, and their respective coefficient of determinations, R^2. Correlation coefficients were 0.893, 0.957, 0.929, and 0.973. **(B)** The correlation between responses on ERRγ LBD and nontarget surfaces, with potential specific ERRγ LBD binders lying above the correlation line (R = 0.83), indicated in purple. **(C)** A plot of the signal on the ERRγ LBD surface against the associated specificity ratio, defined as the response on ERRγ LBD surface divided by the response on nontarget surface. Potential specific binders show responses on the ERRγ LBD surface of between 200 and 350 pm and a specificity ratio of >0.9 (mean + 3×SD). *Note*: In these experiments, addition of all samples caused an increase of 0.5% DMSO, and hence the minimum response is about 130 pm.

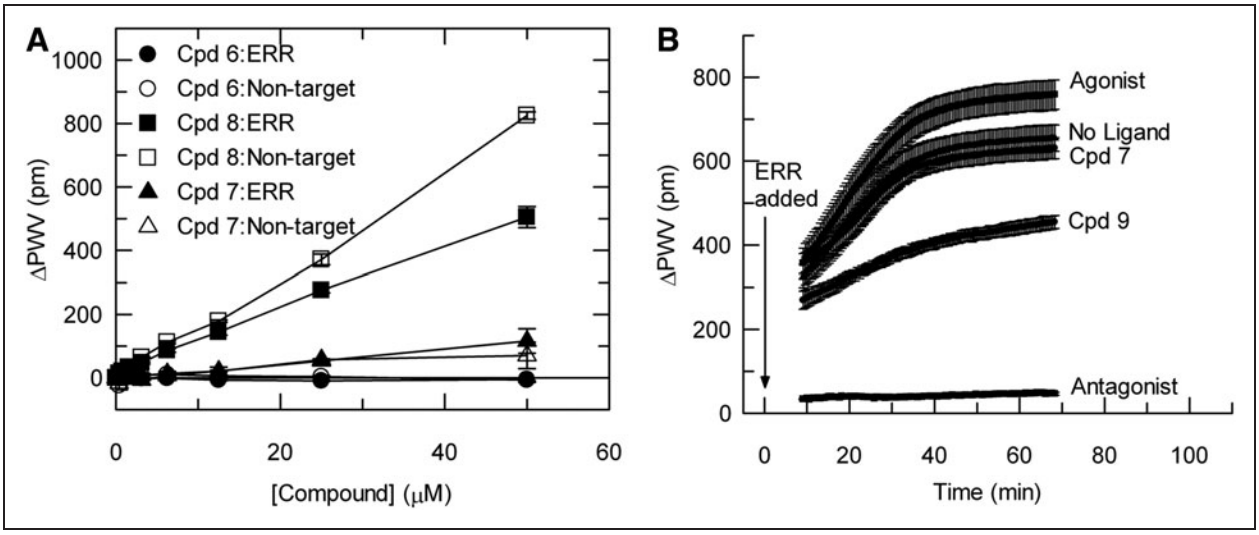

Fig. 8. Characterization of potential hits. **(A)** Dose–response curves for three of the potential hits on ERRγ LBD and nontarget surfaces. Wells of a 384-well GA3 sensor were coated with ERRγ LBD (final level after wash 9,300 ± 200 pm, $n = 384$), blocked with SRU-G, and equilibrated in Assay Buffer supplemented with 1% DMSO, and a baseline was taken. In parallel, another sensor was prepared in the absence of ERRγ LBD (nontarget). Dilution series of compounds 6, 7, and 8 were made in the same buffer and added to both surfaces in quadruplicate to give the indicated final concentrations. The BIND responses ± SD ($n = 4$) after 20 min are shown. The calculated signal for saturating binding to ERRγ LBD of a 1:1 binding ligand of M_r 350 is 120 pm. **(B)** The effect of two potential hits on ERRγ LBD binding to RIP. Wells of a 96-well SA plate were coated with b-RIP (ΔPW = 201 pm) or treated in parallel without b-RIP. The plate was then equilibrated with Assay Buffer containing 0.1% DMSO, a baseline recorded, and emptied. About 1 μL of a 10 mM solution in DMSO of Agonist, Antagonist, or potential hit, or 1 μL of DMSO (no ligand control), were added to 1 mL of 1.25 μM ERRγ LBD in Assay Buffer. After 10 min, 50 μL of each was added. The time-course of BIND response was recorded and that on the RIP surface is shown for the Agonist, Antagonist, and no ligand control, and for compounds 7 and 9 as ΔPWV ± SD (n = 5) at each time-point. The data at each time-point were referenced to parallel additions to the surface without RIP on which a maximum response of 48 pm was seen.

stocks became available of all 9 primary hit compounds, they were freshly dissolved in DMSO and tested for effect on ERRγ LBD binding to b-RIP sensor. The time-courses of binding in the presence and absence of two compounds (10 μM) are shown in *Figure 8B*. In this setup, ERRγ LBD binding gave an average signal of 705 pm on a b-RIP surface, compared to 48 pm in the absence of b-RIP. A standard Agonist gave a 16% increase in signal, whereas 10 μM standard Antagonist produced a 92% reduction in bRIP-dependent ERRγ LBD signal. Two compounds showed nonspecific binding to the surface, seen as an increased signal on both the control and b-RIP-coated wells. Only one (compound 9) showed an experimentally significant effect on ERRγ LBD binding, causing a 31% reduction in the b-RIP-dependent ERRγ LBD signal, making it a weak antagonist. The biochemical and biological effects of these compounds were not pursued further (see Discussion)

DISCUSSION AND CONCLUSIONS

The work presented here illustrates the utility of plate-based biosensors in drug discovery for a challenging model drug target. This label-free technology allowed rapid development and validation of multiple assay formats. Target tractability was determined in <1 day and a validated screening format prepared in <1 week. The present biosensor allowed qualitative and quantitative analysis of the biochemical interactions of the binary and ternary complexes between nuclear receptor, corepressor peptide, and small molecule agonists and antagonist. The biosensor real-time monitoring gave information on time-courses and kinetics that provided mechanistic insights as well as ensuring that equilibrium binding had been achieved. Plate-based biosensors are particularly appropriate for directly measuring equilibrium binding. The 96- to 384- or 1536-well sensor plates can be used to monitor many parallel samples as in a primary screening process giving both "yes/no" binding answers as well as stoichiometry and other mechanistic information.

In the following sections, we discuss technical, practical, and economic aspects that may impact on decisions for when, how, and if to utilize this type of technology.

Reagent Immobilization

Specificity of a biosensor requires immobilization of one component of the interaction. Moreover, the amount and functional quality of the immobilized component defines the detection limit for binding. This is particularly critical for detection of low-molecular-weight ligands. The signal obtained from ligand binding is defined by these factors: first, by the amount of ligand bound, which, in turn, is proportional to the amount of immobilized target; second, by the proportion of the immobilized target that is functional in ligand-binding; third, by the stoichiometry of the interaction; fourth, by the ratio of the M_r of the ligand to that of the immobilized target. With

the technology described here, a ΔPWV of 10 pm represents a signal fivefold greater than noise. To obtain this signal with a saturating concentration of ligand of M_r 350 on a surface of ERRγ LBD of M_r 26400 would require ERRγ LBD to be 100% functional and immobilized to a level of 754 pm. In a screen, or in a dose–response curve, the ligand will not be saturating and hence 5–10-fold higher levels of target are required to be immobilized. If the ligand is of lower M_r, or the target is of higher M_r; then, in either case proportionally more protein will need to be immobilized. Hence, a detection limit is seen which depends upon both the M_r of the ligand, and that of the target and on the ability to immobilize the target in appropriate amounts and functional quality.

To date, no chemistry guarantees successful immobilization for all targets, and thus several surfaces are required to address the full range of targets. Immobilization results in the potential for perturbation of function or apparent activity, through steric or electrostatic effects and also through kinetic constraints caused by reduced rates of diffusion (mass-transport limitation). Users should design experiments to avoid adverse impact. In practice, affinities based on equilibrium binding data are often quite similar to those obtained in solution, being largely unaffected by mass-transport effects.

Typically, only a couple of hours are required to identify a capture surface and reagent conditions (*e.g.*, time, buffer, and concentration) to begin binding experiments (*Figs. 1 and 2*). Through a combination of the immobilization requirements and absolute sensitivity, more target is required in a plate-based biosensor assay as compared with current fluorescence-based technologies.

The optimal density of the bound target will usually differ depending on the type of measurement to be made. Thus, for measurement of small molecule binding, a high-density coating is required to give a sufficiently large signal on binding of a low-molecular-weight ligand. When studying protein–protein interactions, a lower density of coating will reduce the likelihood of steric hindrance, or electrostatic repulsion, on the sensor surface when binding a high-molecular-weight protein, yet will still give a robust signal as the response per mol bound is larger.

Future improvements in sensitivity and surface chemistries in plate-biosensors are likely to result in more generic and optimally orientated immobilization, reduced mass-transport and steric/electrostatic impacts of immobilization, and, importantly, a reduction in the usage of biological material.

Small Molecule Binding

Direct determination of the binding stoichiometry of small molecules using photonic crystal biosensor technology is used in the assay validation stage to ensure that the target is successfully immobilized in a functional state. With another nuclear receptor, direct immobilization using Biacore technology had proven difficult.[18] For most drug targets, the stoichiometry of interaction of a small molecule binder is 1:1 for fully functional targets (cf. *Fig. 2B*). When analyzing compounds of less certain mode of action, this measured stoichiometry becomes important and also provides an alert that there could be a significant nonspecific interaction, providing opportunity to eliminate a compound that may have been a false hit in inhibition assays. Quite frequently large stoichiometries are a direct indicator of compounds that might be working through an aggregation mechanism: the "promiscuous" compounds described by Shoichet and others.[25–29]

Although the calculated stoichiometries of binding of Agonist and Antagonist tool compounds were both close to 1:1, they differed significantly from each other (*Figs. 2 and 3*). It is attractive to think that this apparent discrepancy results from differences in the induced conformational change between agonist and antagonist molecules.[23]

Further, the time-courses of binding of small molecules often give more mechanistic information. Association or dissociation rates that are unexpectedly low, based on knowledge of the target's biochemistry and affinity, are often associated with nonspecific binding responses,[30] such as with compounds like those identified by Shoichet[25–28] that interact with a target surface to give a local denaturing effect. Alternatively, they could also correspond to bona fide specific binders that may trigger a slow structural rearrangement in the target protein. In the case of this nuclear receptor, binding of standard compounds, known to be specific binders, showed some time dependence (though still faster than that shown by some aggregating compounds) (*Fig. 4A*). This is likely a consequence of the large conformational changes that the incompletely folded isolated NR ligand-binding domains undergo when complexed with ligands.[23]

Mechanistic Considerations

The assay format with ERRγ LBD immobilized (*Figs. 1–4*) had a lower functional activity of ERRγ LBD than in the inverted assay with immobilized b-RIP peptide (*Figs. 5 and 6*). The former assay had the benefit of readily showing direct binding of low M_r ligands (*Figs. 1–4*), and then subsequently monitoring the impact of bound ligand on RIP binding (*Fig. 4*). The second format had the benefit of a greater dynamic range for indirect-binding assays that can detect antagonists (mutually exclusive, competitive) binders or agonists that stabilize a ternary complex (*Figs. 5 and 6*). Hence, though both assays could be used to show that addition of an antagonist resulted in a time-dependent removal of RIP from ERRγ LBD and addition of an agonist caused a significant increase in signal from RIP binding to ERRγ LBD, the second format was advantageous for quantitative analysis.

The data obtained suggest that the observed effects of Agonist on RIP binding to immobilized ERRγ LBD were caused by combinations of changes in functional activity, kinetics, and affinity of ERRγ LBD for RIP. Agonist can increase the rate of binding and hence the effects of Agonist can be amplified under nonequilibrium conditions. In the experiment in *Figure 4*, with ERRγ LBD immobilized, the Agonist increased the affinity of ERRγ LBD for RIP. However, in the experiment in *Figure 6*, where RIP is immobilized, the Agonist had no effect on affinity. With RIP immobilized, the affinity for ERRγ LBD was 20–30-fold higher than with ERRγ LBD immobilized (*Figs. 4 and 6*). In both formats, Agonist appeared to increase the maximal amount of

ERRγ LBD.RIP complex that could be formed (*Figs. 4F and 6C*). With ERRγ LBD immobilized, steric hindrance may occur or structural rearrangements may be prevented, thereby reducing the apparent affinity for RIP (*Fig. 4*), but apparently still allowing the Agonist to pull the ERRγ LBD into a more functionally active state. Clearly, more detailed studies would be needed to elucidate the full mechanism of the Agonist.

The combination of different assay formats on one platform provides breadth in discovering and characterizing small molecules that modulate the function of targets with the complexity of a nuclear receptor. This approach can readily be extrapolated to other difficult to assay or complex targets that might include nucleic acid interacting targets (*e.g.*, topoisomerases, polymerases, telomerases, and integrases), catalytically inactive enzymes (*e.g.*, unactivated kinases), or catalytically unstable enzymes (*e.g.*, cyclooxygenase) and protein–protein interactions.[5,12,13]

Time Courses and K_d in Plate-Based Biosensors, as Compared to Flow Biosensors

Flow-based biosensors, such as the Biacore implementation of SPR, have become the gold standard for label-free measurements of association and dissociation phases. Indeed, SPR studies for direct binding of ligands to nuclear receptor ligand-binding domains have been reported,[16–18] though these methods have not been reported with ERRγ. Some of the more significant differences between flow-SPR and the plate-based biosensors employed here are detailed here.

In both technologies, on- and off-rate experiments can be rate-limited by mass transport. In the absence of continued mixing or flow, mass-transport limitation may increase in plate-based biosensors. There is relatively little difference in the mass-transport through the matrix, but the rate of diffusion through the well volume itself becomes a significant factor. In a flow system, contact times with ligand (analyte) are typically in the second to minute time scales, and high flow rates and small cell volumes are required to reach rapid equilibrium (steady state). In contrast in a plate system, contact times can be varied from seconds to hours, or even days; hence, for affinity measurements based upon equilibrium binding, bulk diffusion rates become irrelevant. In practice, on a plate biosensor with an accessible, low-density surface with slow binding, kinetic constants can also be measured without flow or continuous mixing. For off-rates, the large volume of the well gives effective dissipation of displaced ligand, particularly in conjunction with addition of a competing ligand with a fast on-rate.

Importantly, small drug molecules diffuse sufficiently fast that diffusion limitation is not usually an issue on plates. Thus, time-courses can allow distinction from mechanistically unusual situations, such as nonspecific binding, in a similar way as reported with flow-SPR.[30]

In a flow system, a ligand (analyte) is continually replaced with a fresh solution, such that in many cases the concentrations of total ligand and of free ligand are identical; this can simplify analysis of both kinetic and steady-state (equilibrium) measurements. However, in a microplate biosensor well, depletion of ligand occurs by binding to the immobilized target, and the shape of equilibrium dose–response curves can depend on the amount of target immobilized. Hence, plate systems typically have a tight-binding lower limit for K_d. The models used for curve-fitting here explicitly take this into account by utilizing an estimate of the total amount of target in the well.

It should be noted that flow systems typically also have a limit for steady-state binding with low K_d interactions, but in this case it is for kinetic reasons; this arises from the low concentrations, as required to give a full dose–response curve, giving such low association rates that they are experimentally inaccessible.

Very importantly in screening, nonspecific binders, such as slowly dissociating aggregators, have no impact on assay results for other compounds because of the parallel assays that occur in a high-density microplate, whereas in an automated flow system, any compound that either damages the target, or does not rapidly dissociate, during the wash phase, renders useless all subsequent data.

It should also be noted that the parallel nature of the assay on microplate biosensors reduces not only assay time but also assay development time as compared to traditional flow biosensors. In the latter, the target surface needs to be regenerated many times, and hence time and effort is required to ensure surface stability over many hours or often days. This can be a major issue with less stable targets. However, on plate biosensors the target surface only requires functional stability for a single use and for <2 h.

Primary Screening Assay

Assays based on immobilized RIP have several advantages over assays based on immobilized ERRγ LBD in terms of dynamic range and nonspecific binding. However, a key aim of this study was to investigate a format that could be used for a true orphan target, and in particular one without any well-defined ligands. The immobilized ERRγ LBD assay format provided a model system to give the confidence that the technology can be used in a primary screening situation for difficult to assay targets. The BIND assay technology was validated by acceptable hit-rate, throughput, and standard assay-quality parameters. Moreover, the physicochemical properties of those compounds selected were generally drug-like in terms of M_r, clogP, calculated molar refractivity, numbers of heavy atoms and aromatic rings, and total polar surface area.[24] The mean and ranges of these properties were similar to the those of the screening set and also of the two standard compounds. A fear that direct-binding label-free assays might give an unacceptably high apparent hit rate were allayed, as the hit rate was low, and the proportion being false-positives was similar to traditional methods. The Robustness sample set size was such that it was unlikely that there would be any significant number of specific-site binding hits to this challenging target. Hence it is not surprising that only a single compound was found that had an effect on ERRγ LBD function in reducing RIP binding, and even this might have been due to a denaturation effect. Since this compound was of low potency and had the least lead-like physicochemical properties (M_r of 483, clogP of 5.77 and 34 heavy atoms) of the 9 hit

compounds, further biochemical analysis to confirm its mechanism was not undertaken.

These data gave us confidence that these assays and the underlying technology had the capability of finding genuine ERRγ LBD modulators if used in screening a full compound collection or a nuclear receptor-focused set. Compounds identified as binding to the nuclear receptor, and hence with the potential to modulate receptor function *in vivo*, would have been further tested in cell-based model assays that monitored ERRγ function. The primary readout would have been an ERRγ-dependent transcriptional activity. This type of long-term readout requires many biochemical processes and hence is prone to false-positives. The single potentially active compound did not have the potency to warrant testing in such a cell-based assay and would have required lead optimization chemistry to achieve this. As this target was chosen primarily as a model biochemical system for an orphan receptor, no further follow-up was performed. However, the present model has subsequently been taken a step further, and the ligand binding domain of an orphan nuclear receptor for which there were no validated specific binders has been used in a real screening campaign using BIND as the primary assay method.[31] This target had previously been refractory to hit identification by classical indirect biochemical and cell-based screening methods. The assay behaved very similarly to the ERRγ LBD validation described here giving, again, very acceptable screening statistics and numbers of active compounds.

Signal Specificity

The generic nature of the detection principle, that is, refractive index or mass has the obvious advantage of giving a generic readout applicable to nearly every biological interaction and specificity, becomes an important consideration.

Signal specificity is driven by target immobilization. However, in practice it is not uncommon for some nonspecific responses to also be present.

These primarily arise from bulk effects, such as changes in bulk temperature or bulk composition, and from nonspecific binding. Bulk effects, the nature of which is easy to understand as they are governed by simple physical constants, are effectively dealt with by minimization through appropriate experimental design and, when appropriate, software-based referencing to control wells.

By definition, nonspecific binding is not a defined process, and so can be more complex to deal with. Experimental minimization can be achieved by appropriate blocking agents, or additives in the assay medium. Beyond that, control (reference, nontarget) surfaces can be utilized, but they need to be designed with care and the derived data used with caution. Designing a surface that differs from another by the absence of specific binding sites is practically easy. However, designing that surface to retain identical nonspecific interactions is difficult. This was illustrated in *Figure 3*, where a nontarget surface clearly has different nonspecific response to a small molecule than a target, saturated with that ligand. It is likely that the high ERRγ LBD density removes many nonspecific binding sites by changing the physicochemical nature of the surface. Because of this, data were analyzed by assuming that binding followed a 1:1 isotherm + nonspecific binding proportional to the compound concentration, which gave consistently better results than subtracting binding on a reference surface. This has proved to be a highly generic way of analyzing dose–response data, and minimizes any requirement for performing or interpreting, parallel, or replicate assays on target and reference surfaces.

In practice, we have found that differentiation between specific and nonspecific responses can be made by utilizing an appropriate combination of criteria, such as examination of stoichiometry, time-course, concentration–response curves, use of nontarget surfaces, and competition experiments. The detection of nonspecific binders can also be used to our advantage in detecting those aggregating compounds, described above, that can interact with the surface of a target protein or other components of a screening assay and cause mechanistically unacceptable inactivation.[25–29]

Economics

One current limitation of label-free methodologies on HTS is cost/well when compared with a pre-existing fluorescence-based uHTS format. For true comparability, the whole debit to the organization needs to be calculated on a more comprehensive basis than cost/well. In particular, development of an appropriate labeled reagent, and the economics of that reagent is obviated.

Conclusion

The data presented here go toward validating optical plate-based label-free technology within the drug discovery process. We would specifically highlight these areas in which traditional methods have more limitations, and label-free should have maximal impact: fragment-based screening, novel hit identification strategies, hit (in)validation, orthogonal readout to a screen anticipated to have false-positives, hit-to-lead, lead optimization support, orphan, and nonenzymatic targets. Label-free applications can enable, complement, or simplify some of the methodological approaches currently available. In principle, the universal principle of detection (label-free, any-target) created the opportunity for direct label-free assays for small compounds binding to any target. The amenability of plate-based biosensors to classical HTS infrastructure in a cost-effective manner opens the possibility of making such assays more widely accessible and opening up new classes of therapeutic targets for the drug discovery process.

ACKNOWLEDGMENTS

Authors want to acknowledge all members of the label-free team (screening, automation, IT, assay development, and compound management) at GSK Tres Cantos for their contributions to the experimental work, as well as Emilio Diez and Robert Hertzberg for their endorsement to assess technical feasibility of label-free and to Denise Lowe in article preparation.

AUTHOR DISCLOSURE STATEMENT

P.N.L. performed this work as a Consultant to SRU Biosystems. L.G.L. was a director to SRU Biosystems at the time of the work.

REFERENCES

1. Venter C, *et al.*: The sequence of human genome. *Science* 2001;291:1304–1351.
2. Comley J: Label-free detection: new biosensors facilitate broader range of drug discovery applications. *Drug Discov World* 2004;5:63–74.
3. Chung C-W, Lowe PN: Biophysical methods: mechanism of action studies. In: *Structure-Based Drug Discovery* (Jhoti H, Leach AR, eds.), Springer, Dordrecht, The Netherlands 2007, 155–200.
4. Comley J: HTStec's surveys: binding and cell-based label-free detection trends. *Drug Discovery World* 2008;9(3):77–88. Available at: www.htstec.com/.
5. Martin J: High-throughput optical label-free in early drug discovery: from biomolecular interactions to cellular phenotypes. *Am Drug Discov* 2008;3:12.
6. Huber W: A new strategy for improved secondary screening and lead optimization using high-resolution SPR characterization of compound-target interactions. *J Mol Recognit* 2005;18:273–281.
7. Perspicace S, Banner D, Benz J, Muller F, Schlatter D, Huber W: Fragment-based screening using surface plasmon resonance technology. *J Biomol Screen* 2009;14:337–349.
8. Hämäläinen MD, Zhukov A, Ivarsson M, Fex T, Gottfries J, Karlsson R, Björsne M: Label-free primary screening and affinity ranking of fragment libraries using parallel analysis of protein panels. *J Biomol Screen* 2008;13:202–209.
9. Cunningham BT, Li P, Schulz S, Lin B, Baird C, Gerstenmaier J, Genick C, Wang F, Fine E, Laing L: label-free assays on the BIND system. *J Biomol Screen* 2004; 9:481–490.
10. Chan LL, Pineda MF, Heeres J, Hergenrother P, Cunningham BT: General method for discovering inhibitors of protein-DNA interactions using photonic crystal biosensors. *ACS Chem Biol* 2008;3:437–448.
11. Cunningham BT, Laing LL: Microplate-based label-free detection of biomolecular interactions: applications in proteomics. *Expert Rev Proteomics* 2006;3:271–281.
12. Fang Y, Fang J, Tran E, Xie X, Hallstrom A, Frutos AG: High-throughput analysis of biomolecular interactions and cellular responses with resonant waveguide grating biosensors. In: *Label-Free Biosensors: Techniques and Applications* (Cooper MA, ed.), Cambridge University Press, Cambridge, United Kingdom, 2009, 206–221.
13. Minor LK: Label-free cell-based functional assays. *Comb Chem High Throughput Screen* 2008;11:573–580.
14. Tremblay AM, Giguere V: The NR3B subgroup: an ovERRview. *Nucl Recept Signal* 2007;5:e009.
15. Alaynick WA, Kondo RP, Xie W, He W, Dufour CR, Downes M, Jonker JW, Giles W, Naviaux RK, Giguere V, Evans RM: ERRgamma directs and maintains the transition to oxidative metabolism in the postnatal heart. *Cell Metab* 2007;6:13–24.
16. Rich RL, Hoth LR, Geoghegan KF, Brown TA, LeMotte PK, Simons SP, Hensley P, Myszka DG: Kinetic analysis of estrogen receptor/ligand interactions *Proc Natl Acad Sci U S A* 2002;99:8562–8567.
17. Rich RL, Myska DG: Resolving estrogen receptor agonist/antagonist kinetics using Biacore's SPR technology. *Biacore J* 2002;2:4–6.
18. Scaffold-class analysis of lead compounds by SPR using a combination of screening and kinetic characterization; Biacore® S51 analyzes 200 lead compounds targeted against human estrogen receptors. *Biacore Application Note 26,* 2004.
19. Zuercher WJ, Gaillard S, Orband-Miller LA, Chao EYH, Shearer BG, Jones DG, Miller AB, Collins JL, McDonnell DP, Willson TM: Identification and structure-activity relationship of phenolic acyl hydrazones as selective agonists for the estrogen-related orphan nuclear receptors ERRα and ERRγ. *J Med Chem* 2005;48:3107–3109.
20. Coward P, Lee D, Hull MV, Lehman JM: 4-Hydroxytamoxifen binds to and deactivates the estrogen-related receptorγ. *Proc Natl Acad Sci* 2001;98:8880–8884.
21. Thompson G, Owen D, Chalk PA, Lowe PN: Delineation of the Cdc42/Rac-binding domain of p21-activated kinase. *Biochemistry* 1998;37:7885–7891.
22. Lowe PN, Gerstemaier J, Laing L, Fekkes P: The BIND biosensor technology: label-free detection for small molecule binding. [Poster P04060] Poster presented at the 11th Annual Conference of the SBS, Geneva, September 2005.
23. Koide A, Abbatiello S, Rothgery L, Koide S: Probing protein conformational changes in living cells by using designer binding proteins: Application to the estrogen receptor. *Proc Natl Acad Sci U S A* 2002;99:1253–1258.
24. Hann MM, Leach AR, Harper G: Molecular complexity and its impact on the probability of finding leads for drug discovery. *J Chem Inf Comput Sci* 2001;41:856–864.
25. McGovern SL, Helfand BT, Feng B, Shoichet BK: A specific mechanism of nonspecific inhibition. *J Med Chem* 2003;46:4265–4272.
26. Coan KE, Maltby DA, Burlingame AL, Shoichet BK: Promiscuous aggregate-based inhibitors promote enzyme unfolding. *J Med Chem* 2009;52:2067–2075.
27. Coan KE, Shoichet BK: Stoichiometry and physical chemistry of promiscuous aggregate-based inhibitors. *J Am Chem Soc* 2008:130:9606–9612.
28. Feng BY, Shelat A, Doman TN, Guy RK, Shoichet BK: High-throughput assays for promiscuous inhibitors. *Nat Chem Biol* 2005;1:146–148.
29. Ryan AJ, Gray NM, Lowe PN, Chung C: Effect of detergent on "promiscuous" inhibitors. J Med Chem 2003;46:3448–3451.
30. Gianetti AM, Koch BD, Browner MF: Surface plasmon resonance based assay for the detection and characterization of promiscuous inhibitors. *J Med Chem* 2008;51:574–580.
31. Roa AM, Vela L, Sandberg E, Lowe P, Laing L, Sobrino M, Martin JJ: Small molecule drug screening using a label-free assay on the BIND system. [Poster 238] Poster presented at Miptec, Basel, October 2008.

Address correspondence to:
Peter N. Lowe, PhD
Biomolecular Interactions Consultancy
3 Danesbury Park, Hertford SG14 3HX
United Kingdom

E-mail: peter.lowe@dsl.pipex.com